

Data-Driven Decentralized Optimal Power Flow

Roel Dobbe, Oscar Sondermeijer, David Fridovich-Keil, Daniel Arnold, Duncan Callaway and Claire Tomlin

Abstract—The implementation of optimal power flow (OPF) methods to perform voltage and power flow regulation in electric networks is generally believed to require communication. We consider distribution systems with multiple controllable Distributed Energy Resources (DERs) and present a data-driven approach to learn control policies for each DER to reconstruct and mimic the solution to a centralized OPF problem from solely locally available information. Collectively, all local controllers closely match the centralized OPF solution, providing near-optimal performance and satisfaction of system constraints. A rate distortion framework facilitates the analysis of how well the resulting fully decentralized control policies are able to reconstruct the OPF solution. Our methodology provides a natural extension to decide what buses a DER should communicate with to improve the reconstruction of its individual policy. The method is applied on both single- and three-phase test feeder networks using data from real loads and distributed generators. It provides a framework for Distribution System Operators to efficiently plan and operate the contributions of DERs to active distribution networks.

I. INTRODUCTION

Historically, low and medium voltage distribution networks facilitated uni-directional, predictable power flow from substations to end customers. By conservatively oversizing cables and control equipment, Distribution System Operators (DSOs) could deal with peak and contingency scenarios safely, while requiring limited sensing and control actions. Gradual changes in the network were typically dealt with by a *fit-and-forget* approach, through capital intensive network reinforcements that could satisfy the needs for decades to come.

This paradigm was first challenged by the rapid advent of Distributed Generation (DG), mostly through photovoltaic (PV) systems, leading to new risks of over-voltage, reverse flow, and thermal overloads, especially at times of high DG and low consumption [38]. The subsequent adoption of electric vehicles (EVs), battery storage and other Distributed Energy Resources (DERs), increasingly interfaced by controllable electronic power inverters, has shaped a new reality with more challenging quickly diversifying power flow and voltage dynamics requiring a new control paradigm.

Many Distribution System Operators (DSOs) are testing ways to prevent expensive network updates by exploiting DERs and their sensing and actuation capabilities to provide *distributed energy services* (DES) to enable *active distribution networks*. In DES, DERs are embraced (1) to compensate for the negative effects of DG and EVs thereby allowing higher levels of penetration, and (2) to distribute and diversify capital investments on the grid *both in space and time*, to align closer

with actual changes that occur organically. The latter benefit can dramatically decrease capital costs, as larger updates tend to be more conservative due to longer and more uncertain planning horizons [24].

A. Relevant Advances in Active Distribution Networks

Earlier efforts to address voltage and power flow problems related to higher penetrations of DERs aimed at developing *decentralized control based on local information* [10, 23, 36, 40]. These use heuristics to adjust reactive power output at each inverter based on the local voltage have shown promise in their ability to reduce voltage variability, but suffer from extensive tuning, which is impractical for larger networks with many inverters. In addition, these methods yield suboptimal control signals and have been shown to not guarantee the satisfaction of critical system constraints [11]. A step further, we find methods that consider a control theoretic formulation emulating proportional [26] or integral control [41]. Relatedly, some consider the use of sensitivities between controllable variables and relevant quantities in the network such as voltage levels or branch flows [32, 30, 9]. Lastly, [41] proposes a simple localized optimization framework aiming to track a local voltage reference, and provides necessary conditions that show that localized control does not converge and may not be stable for longer and more heavily loaded networks.

The emerging need for active distribution grids also motivated the use of Optimal Power Flow (OPF) for Distribution Operation to enable *optimization-based control based on system-wide information* [16]. OPF refers to solving an optimization problem that minimizes some economic or operational objective subject to power flow and other relevant system constraints. Traditionally, OPF is used *offline* as a design tool for network upgrades to size and place equipment, as proposed for capacitor planning in [5, 4], or as a planning tool to schedule the dispatch of generators and control equipment. With theoretical advances in optimization [3, 25] overcoming the lack of convergence guarantees [29], the implementation of OPF in an *online* setting has been a popular research area in recent years.

The inherent lack of communication infrastructure in distribution networks subsequently motivated various efforts to implement OPF in a *distributed* fashion, relying on agent-to-agent communication, such as via consensus algorithms [42] or dual decomposition [8, 13, 39]. Recent work in extremum-seeking showed that model-free optimization is possible with provable guarantees for convergence and convexity for a variety of distribution feeder objective functions over a broad range of power flows [1]. Despite the elegance of distributed solutions, the necessary communication infrastructure is still a steep investment at the scale of transforming distribution networks. It remains a challenge to understand what can be done with

R. Dobbe, D. Fridovich-Keil and C. Tomlin are with the Department of Electrical Engineering & Computer Sciences, UC Berkeley, Berkeley, CA 94702 USA e-mail: dobbe@berkeley.edu. D. Arnold is with the Grid Integration Group at Lawrence Berkeley National Laboratory. D. Callaway is with the Energy & Resources Group at UC Berkeley.

Manuscript received June 2018.

minimal investments in assets and communication infrastructure by fully exploiting existing infrastructure and the capabilities of naturally arising DERs.

B. Approach and Contributions

We propose a method that decentralizes the implementation of optimal power flow (OPF) based on machine learning to regulate voltage and power flow in distribution grids without the need for communication. The contribution of this work lies in combining the “best of both worlds” by exploiting the complexity of OPF and using machine learning to *learn* simpler controller for each DER that can *locally mimic or reconstruct* the actions from a system-wide OPF controller determined in simulation. As such, the method provides a data-driven approach to tuning controllers that is fully automatic, relying on historical and simulated load and generation data and a model of the network.

The approach consists of four steps. First, for a specific network with a set of controllable DERs, we retrieve data points for loads and generators for T different scenarios, collected over an extended period of time, typically collected by advanced metering infrastructure (AMI) or from simulations. Second, for all scenarios, we run a centralized optimal power flow computation to understand how a group of DERs best minimizes a collective objective by adjusting real and/or reactive power injections, given certain capacity, operational and safety constraints. Third, for each individual DER, we use supervised learning to determine a function that relates its *local* measurements to its optimal power injections, as determined by OPF. Last, we implement these functions as controllers on the system to determine power injections based on a new local measurement that collectively mimic a centralized OPF scheme.

As such, we bridge control techniques based on local information with those based on system-wide optimization, thereby making contributions that overcome their respective limitations. Firstly, our method yields close-to-optimal results for various OPF objectives, for both single-phase and unbalanced three-phase networks (see supplementary materials). As such, the method respects constraints on voltage, equipment specifications and power capacity. Secondly, the implementation of decentralized OPF is data-driven and needs little or no real-time communication, avoiding expensive investments in infrastructure, controller tuning and maintenance. Thirdly, our method has the ability to operate in congruence with the existing *legacy control equipment*, such as load tap changers and capacitor banks, making the method relevant in contexts where operators or other autonomous systems make real-time control decisions. Fourthly, the controller’s strict dependence on disturbance variables not affected by control actions circumvents stability issues. Lastly, analyzing the structure of the learned controllers in terms of: (a) what local measurements are selected by the machine learning algorithm and (b) which nodes are optimal to communicate with in order to improve the reconstruction, provides new insights in the complexity of operating distribution networks with optimal power flow methods.

This learning-based optimization approach was first proposed for reactive power control in [37], further formalized with information theory in [15], and recently applied to design voltage-reactive power droop-curves in [6].

II. OPTIMAL POWER FLOW

Single-Phase Power Flow Modeling

We consider the full nonlinear *DistFlow* model [5] for single-phase networks. We model a network $\mathcal{G} := (\mathcal{N}, \mathcal{E})$ with buses or nodes \mathcal{N} and edges or branches \mathcal{E} . The branch flow equations are

$$P_{mn} = r_{mn}\ell_{mn} + p_n^c - p_n^g + \sum_{(n,k) \in \mathcal{E}, k \neq m} P_{nk}, \quad (1)$$

$$Q_{mn} = x_{mn}\ell_{mn} + q_n^c - q_n^g + \sum_{(n,k) \in \mathcal{E}, k \neq m} Q_{nk}, \quad (2)$$

$$y_m - y_n = 2(r_{mn}P_{mn} + x_{mn}Q_{mn}) - (r_{mn}^2 + x_{mn}^2)\ell_{mn}, \quad (3)$$

$$\ell_{mn} = \frac{P_{mn}^2 + Q_{mn}^2}{y_m}, \quad \forall (m, n) \in \mathcal{E}, \quad (4)$$

where P_{mn}, Q_{mn} denote the real and reactive power flowing out of node m towards node n , p_n^c and q_n^c are the real and reactive power consumption at node n , p_n^g and q_n^g are the real and reactive power generation at node n , $y_n := V_n^2$ is the squared voltage magnitude, and $\ell_{mn} := I_{mn}^2$ is the squared current magnitude on branch (m, n) . r_{mn} and x_{mn} are the resistance and reactance of branch (m, n) . Here, we assume the nodal injections to be constant power and not sensitive to voltage or current fluctuations. We assume we are given a subset $\mathcal{C} \subset \mathcal{N}$ of buses that are equipped with a controllable source or load. We consider different controller architectures that can deliver *both* real and reactive power u_i^p, u_i^q . Whether these are available depends on the controllable parts of the inverter-interfaced system. For instance, a bus n may have an uncontrollable load p_n^c, q_n^c , and controllable real and reactive power capacity, which means $u_n^p := p_n^g, u_n^q := q_n^g$.

Single-Phase Optimal Power Flow Framework

We consider the following optimal power flow formulation:

$$\min_{\mathbf{z}} f_o(\mathbf{z}) \quad (5)$$

$$\text{s.t. } (1) - (3),$$

$$\ell_{mn} \geq \frac{P_{mn}^2 + Q_{mn}^2}{y_m}, \quad \forall (m, n) \in \mathcal{E}, \quad (6)$$

$$\text{capacity constraints on } u_i^p, u_i^q,$$

$$\underline{y} \leq y_n \leq \bar{y}, \quad \forall n \in \mathcal{N}, \quad (7)$$

$$\mathbf{z} = (y_n, \ell_{mn}, P_{mn}, Q_{mn}, u_i^p, u_i^q),$$

$$\forall n \in \mathcal{N}, \quad \forall (m, n) \in \mathcal{E}, \quad \forall i \in \mathcal{C}.$$

In our case studies in Section V, we optimize various objectives relevant in distribution grid operations.

$$f_o := \alpha \sum_{(m,n) \in \mathcal{E}} r_{mn}\ell_{mn} + \beta \sum_{n \in \mathcal{N}} (y_n - y_{\text{ref}})^2 + \gamma (P_{01}^2 + Q_{01}^2). \quad (8)$$

Firstly, the convex relaxation requires an objective convex in the squared current magnitude ℓ_{mn} to ensure the solution lies on the feasibility boundary of the inequality constraint (6), thereby satisfying the original equality constraint (4), as explained in [28]. We use this fact to address real power losses by minimizing $r_{mn}\ell_{mn}$. Secondly, we minimize voltage deviations from a reference and voltage variability due to the intermittent nature of generation and consumption. This objective aims to actively keep the voltage in a safe and desirable operable regime. Lastly, we aim to make a network *self-sufficient* by minimizing power delivered from the transmission grid, injected at the top of a radial network, thereby maximizing the use of distributed energy resources to provide loads nearby. α, β, γ denote trade-off parameters (these could take on the form of a financial price), and y_{ref} the reference voltage throughout the network. The nonlinear equality constraint (4) is relaxed to (6), enabling a convex second order cone program [28]. Equation (7) formulates the responsibility of American utilities to maintain service voltage within $\pm 5\%$ of 120V as specified by ANSI Standard C84.1.

Two constraints are included to account for inverter capacity and voltage goals. Each controller $i \in \mathcal{C}$ is ultimately limited by a local capacity on total apparent power capacity \bar{s}_i . The capacity constraints may be decoupled

$$\underline{p}_i(t) \leq u_i^p(t) \leq \bar{p}_i(t), \quad \underline{q}_i(t) \leq u_i^q(t) \leq \bar{q}_i(t), \quad (9)$$

with $\underline{p}_i, \bar{p}_i$ denoting the lower and upper capacity constraints on nodal power injection. Alternatively, we might consider a *four-quadrant* configuration, which yields a disk constraint,

$$(u_i^p)^2(t) + (u_i^q)^2(t) \leq \bar{s}_i^2(t), \quad (10)$$

Lastly, we consider inverters that also interface a system with local photovoltaic (PV) installation, an electric vehicle (EV) or battery charging system, smart loads or a combination thereof. Due to the nature of these subsystems having some hierarchy of priority, it can happen that the capacity available for the OPF problem is dependent on the scheduling and activity of these other systems. For instance, it is possible the inverter can only deliver/consume reactive power based on the remaining capacity *after* injecting surplus energy from the PV installation into the grid. In this case, the reactive power capacity $\bar{q}_i[t]$ at time t of an inverter is limited by the total apparent power capacity \bar{s} (constant) minus the real power $p_i^g[t]$. As a result, the demand of reactive power does not interfere with real power generation, which is formulated as

$$|u_i^q[t]| \leq \bar{q}_i[t] = \sqrt{\bar{s}_i^2 - (p_i^g[t])^2}. \quad (11)$$

We assume that each inverter has some overcapacity with respect to the maximum real power output, e.g. $\bar{s} = 1.05\bar{p}$.

A. Three-phase Power Flow Modeling

Whereas the use of convex relaxations is well-applicable in single-phase networks, these are not yet robust enough for the more complex OPF formulations for unbalanced three-phase systems. Its development for three-phase networks [13] is hampered by issues of nondegeneracy and inexactness of the semidefinite relaxations [27]. In [34, 7], linear approximations

of the unbalanced power flow are proposed to overcome these challenges and enable three-phase OPF for a broad range of conditions. Here we adopt the modeling developed in [2, 33, 34], which can be seen as an adaptation of the *DistFlow* model [5] to unbalanced circuits, coined the *Dist3Flow* model. We restate part of the model's derivation here to provide sufficient intuition for its use in experiments. In this setting, each node and line segment can have up to three phases, labeled a, b , and c . Phases are referred to by the variables ϕ and ψ , where $\phi \in \{a, b, c\}$, $\psi \in \{a, b, c\}$. If line (m, n) exists, its phases must be a subset of the phases present at both node m and node n .

The current/voltage relationship for a three phase line (m, n) between adjacent nodes m and n is captured by Kirchhoff's Voltage Laws (KVL) in its full (12), and compact form (13):

$$\begin{bmatrix} V_m^a \\ V_m^b \\ V_m^c \end{bmatrix} = \begin{bmatrix} V_n^a \\ V_n^b \\ V_n^c \end{bmatrix} + \begin{bmatrix} Z_{mn}^{aa} & Z_{mn}^{ab} & Z_{mn}^{ac} \\ Z_{mn}^{ba} & Z_{mn}^{bb} & Z_{mn}^{bc} \\ Z_{mn}^{ca} & Z_{mn}^{cb} & Z_{mn}^{cc} \end{bmatrix} \begin{bmatrix} I_{mn}^a \\ I_{mn}^b \\ I_{mn}^c \end{bmatrix} \quad (12)$$

$$\mathbf{V}_m = \mathbf{V}_n + \mathbf{Z}_{mn}\mathbf{I}_{mn} \quad (13)$$

Here, $Z_{mn}^{\phi\psi} = r_{mn}^{\phi\psi} + jx_{mn}^{\phi\psi}$ denotes the complex impedance of line (m, n) across phases ϕ and ψ .

Next, we define the per phase complex power as $\mathbf{S}_{mn}^\phi = \mathbf{V}_n^\phi (\mathbf{I}_{mn}^\phi)^*$, and the 3×1 vector of complex power phasors $\mathbf{S}_{mn} = \mathbf{V}_n \circ \mathbf{I}_{mn}^*$ where \mathbf{S}_{mn} is the power from node m to node n at node n .

$$\sum_{l:(l,m) \in \mathcal{E}} \mathbf{S}_{lm} = \mathbf{s}_m + \sum_{n:(m,n) \in \mathcal{E}} \mathbf{S}_{mn} + \mathbf{L}_{mn} \quad (14)$$

The term $\mathbf{L}_{mn} \in \mathbb{C}^{3 \times 1}$ is a nonlinear and non-convex loss term. As in [18] and [5], we assume that losses are negligible compared to line flows, so that $|L_{mn}^\phi| \ll |S_{mn}^\phi| \quad \forall (m, n) \in \mathcal{E}$. Thus, we neglect line losses, linearizing (14) into (15).

$$\sum_{l:(l,m) \in \mathcal{E}} \mathbf{S}_{lm} \approx \mathbf{s}_m + \sum_{n:(m,n) \in \mathcal{E}} \mathbf{S}_{mn} \quad (15)$$

Now, we define the real scalar $y_m^\phi = |V_m^\phi|^2 = V_m^\phi (V_m^\phi)^*$, the 3×1 real vector $\mathbf{y}_m = [y_m^a, y_m^b, y_m^c]^T = \mathbf{V}_m \circ \mathbf{V}_m^*$. With these definitions, [34] derives the following equations that govern the relationship between squared voltage magnitudes and complex power flow across line (m, n) :

$$\begin{aligned} \mathbf{y}_m &= \mathbf{y}_n + 2\mathbf{M}_{mn}\mathbf{P}_{mn} - 2\mathbf{N}_{mn}\mathbf{Q}_{mn} + \mathbf{H}_{mn} \\ \mathbf{M}_{mn} &= \mathbf{Re}\{\Gamma_n \circ \mathbf{Z}_{mn}^*\}, \mathbf{N}_{mn} = \mathbf{Im}\{\Gamma_n \circ \mathbf{Z}_{mn}^*\}, \end{aligned} \quad (16)$$

where $\Gamma_n = \mathbf{V}_n (1/\mathbf{V}_n)^T \in \mathbb{C}^{3 \times 3}$ represents a matrix with voltage balance ratios across all phases at node n . Hence, we have that $\Gamma_n(\phi, \phi) = 1$ and $\Gamma_n(\phi, \psi) = V_n^\phi / V_n^\psi \triangleq \gamma_n^{\phi\psi}$. Furthermore, $\mathbf{H}_{mn} = (\mathbf{Z}_{mn}\mathbf{I}_{mn}) \circ (\mathbf{Z}_{mn}\mathbf{I}_{mn})^* = (\mathbf{V}_m - \mathbf{V}_n) \circ (\mathbf{V}_m - \mathbf{V}_n)^*$ is a 3×1 real-valued vector representing higher-order terms. Notice that we have separated the complex power vector into its active and reactive components, $\mathbf{S}_{mn} = \mathbf{P}_{mn} + j\mathbf{Q}_{mn}$.

This nonlinear and nonconvex system is difficult to incorporate into a state estimation or optimization formulation without the use of convex relaxations. Following the analysis in [18], we apply two approximations. The first approximation is legitimized by the fact that the high order term \mathbf{H}_{mn}

is negligible, such that $\mathbf{H}_{mn} = [0, 0, 0]^T$. The second approximation assumes that node voltages are “nearly balanced” such that:

$$\Gamma = \begin{bmatrix} 1 & \gamma_n^{ab} & \gamma_n^{ab} \\ \gamma_n^{ba} & 1 & \gamma_n^{bc} \\ \gamma_n^{ca} & \gamma_n^{cb} & 1 \end{bmatrix} = \begin{bmatrix} 1 & \alpha & \alpha^2 \\ \alpha^2 & 1 & \alpha \\ \alpha & \alpha^2 & 1 \end{bmatrix} \forall n \in \mathcal{N}, \quad (17)$$

where $\alpha = 1\angle 120^\circ = \frac{1}{2}(-1 + j\sqrt{3})$ and $\alpha^{-1} = \alpha^2 = \alpha^* = 1\angle 240^\circ = \frac{1}{2}(-1 - j\sqrt{3})$. Applying the approximations for \mathbf{H}_{mn} and Γ_n to (16), we arrive at a linear system of equations:

$$\mathbf{y}_m \approx \mathbf{y}_n + 2\mathbf{M}_{mn}\mathbf{P}_{mn} - 2\mathbf{N}_{mn}\mathbf{Q}_{mn}, \text{ with} \quad (18)$$

$$2\mathbf{M}_{mn} = \dots$$

$$\begin{bmatrix} 2r_{mn}^{aa} & -r_{mn}^{ab} + \sqrt{3}x_{mn}^{ab} & -r_{mn}^{ac} - \sqrt{3}x_{mn}^{ac} \\ -r_{mn}^{ba} - \sqrt{3}x_{mn}^{ba} & 2r_{mn}^{bb} & -r_{mn}^{bc} + \sqrt{3}x_{mn}^{bc} \\ -r_{mn}^{ca} + \sqrt{3}x_{mn}^{ca} & -r_{mn}^{cb} - \sqrt{3}x_{mn}^{cb} & 2r_{mn}^{cc} \end{bmatrix}, \quad (19)$$

$$2\mathbf{N}_{mn} = \dots$$

$$\begin{bmatrix} -2x_{mn}^{aa} & x_{mn}^{ab} + \sqrt{3}r_{mn}^{ab} & x_{mn}^{ac} - \sqrt{3}r_{mn}^{ac} \\ x_{mn}^{ba} - \sqrt{3}r_{mn}^{ba} & -2x_{mn}^{bb} & x_{mn}^{bc} + \sqrt{3}r_{mn}^{bc} \\ x_{mn}^{ca} + \sqrt{3}r_{mn}^{ca} & x_{mn}^{cb} - \sqrt{3}r_{mn}^{cb} & -2x_{mn}^{cc} \end{bmatrix}. \quad (20)$$

We present the full set of equations that comprise a linearized model for unbalanced power flow. We named these the *LinDist3Flow* equations, as developed in [2, 33, 34].

LinDist3Flow Equations for Three-Phase Networks

Per phase node complex load:

$$s_n^\phi(y_n^\phi) = (\beta_{S,n}^\phi + \beta_{Z,n}^\phi y_n^\phi) d_n^\phi + u_n^\phi - j c_n^\phi, \quad (21)$$

$$\forall \phi \in \mathcal{P}_n, \forall n \in \mathcal{N}$$

Branch power flow:

$$\sum_{l:(l,m) \in \mathcal{E}} \mathbf{S}_{lm} \approx \mathbf{s}_m + \sum_{n:(m,n) \in \mathcal{E}} \mathbf{S}_{mn}, \forall m \in \mathcal{N} \quad (22)$$

Magnitude and angle equations:

$$[\mathbf{y}_m \approx \mathbf{y}_n + 2\mathbf{M}_{mn}\mathbf{P}_{mn} - 2\mathbf{N}_{mn}\mathbf{Q}_{mn}]_{\mathcal{P}_{mn}}, \quad (23)$$

$$[\Theta_m \approx \Theta_n - \mathbf{N}_{mn}\mathbf{P}_{mn} - \mathbf{M}_{mn}\mathbf{Q}_{mn}]_{\mathcal{P}_{mn}}, \quad (24)$$

$$\text{with } [\mathbf{M}_{mn} = \mathbf{Re}\{\Gamma\mathbf{Z}_{mn}^*\}, \mathbf{N}_{mn} = \mathbf{Im}\{\Gamma\mathbf{Z}_{mn}^*\}]_{\mathcal{P}_{mn}} \\ \forall (m, n) \in \mathcal{E}. \quad (25)$$

Here, we have embraced a load model with a fixed voltage sensitivity (as parameterized with $\beta_{S,n}^\phi, \beta_{Z,n}^\phi$), with d_n^ϕ denoting demand, $u_n^\phi := u_n^{p,\phi} + j u_n^{q,\phi}$ the controllable power injection and c_n^ϕ a possible capacitor bank.

The accuracy of the approximations in the power and voltage magnitude equations has been investigated in [18] and [31]. In [34], we perform a Monte Carlo analysis to explore the level of error introduced by the voltage angle equation assumptions.

B. Three-phase Optimal Power Flow

Voltage Balancing

Although the *LinDist3Flow* equations allow for a flexible OPF framework comparable to the one presented for single-phase networks above, here we focus on one instance to demonstrate the generalization of decentralized OPF to three-phase

unbalanced systems. We remodel an instance first presented in [33] that demonstrated OPF for balancing voltage magnitudes on an unbalanced radial distribution feeder. This is an important objective as many three phase loads (induction motors for instance) are sensitive to high levels of voltage imbalance. Furthermore, 3-phase voltage regulation equipment may actuate based on single phase measurements, and significant imbalances can lead to improper operation of these devices. The problem is defined as

$$\min_{y_n^\phi, P_{mn}^\phi, Q_{mn}^\phi, u_n^\phi} \sum_{n \in \mathcal{N}} \left[\sum_{\phi \neq \psi} (y_n^\phi - y_n^\psi)^2 + \rho \sum_{\phi} |u_n^\phi|^2 \right] \\ \text{s.t.} \quad (21), (22), (23), \underline{y} \leq y_n^\phi \leq \bar{y}, \\ |u_n^\phi| \leq \bar{u}, \quad \forall n \in \mathcal{N},$$

where $\phi, \psi \in \{a, b, c\}$. The parameter ρ is a penalty on control action set to 0.01. [33] showed the effectiveness of the *LinDist3Flow* model in drastically reducing voltage imbalance across phases, and we will aim to reproduce these results in Section V-A.

III. MACHINE LEARNING

As depicted in Figure 1 (right), we treat the i^{th} agent's optimal action in the centralized problem as a random variable u_i^* , and model its conditional dependence on the global state variables $x = (x_1, \dots, x_{|\mathcal{N}|})$, i.e. $p(u_i^*|x)$, which we assume to be stationary in time. Notice that u_i^* is often a deterministic function of x (if the optimization has a unique solution), in which case $p(u_i^*|x)$ is a singleton distribution. We then restrict each agent i to observe only the i^{th} state variable x_i . Rather than solving this decentralized problem directly, we train each agent to replicate what it would have done with full information in the centralized case. That is, the vector of state variables x is *compressed*, and the i^{th} agent must decompress x_i to compute some estimate $\hat{u}_i \approx u_i^*$. In our approach, each agent learns a parameterized Markov control policy $\hat{u}_i = \hat{\pi}_i(x_i)$ via regression. The $\hat{\pi}_i$ are learned from a data set containing local states x_i taken from historical measurements of system state x and corresponding optimal actions u_i^* computed by solving an offline centralized optimization problem for each x . Figure 2 presents a flow diagram explaining the method.

In the OPF context, the goal of the machine learning procedure is to find a model for each DER $i \in \mathcal{C}$ that closely reconstructs the optimal power injection u_i^* based *solely* on local measurements x_i available at node i . We first construct a *central training set* consisting of power flow scenarios that are representative of future behavior on the grid. This data set can contain historical measurements taken from advanced metering infrastructure (AMI) in the grid, augmented with proxy data for variables that were not measured or for scenarios that did not occur in the past but are anticipated to occur in the future. For example, a load not metered by AMI, may be approximated with an average load profile. Examples of anticipated future behaviors not captured in historical measurements are connections of new electric vehicles or solar installations. These can be simulated and added to the training set. Together, the central training set contains T power flow scenarios augmented with the optimal control

set points $u_i^*[t] \forall i \in \mathcal{C}, t = 1, \dots, T$, which were computed in a centralized OPF problem as defined in Section II.

Regression is now performed for each individual DER, by selecting a *local data set* from the central data set. Here, we deliberately choose to only select exogenous uncontrollable variables d_i that are measured at node i , as depicted in Figure 1 (left). As such, we do not consider states in x_i that are dynamically coupled with the control u_i , thereby circumventing instability arising from controller interactions. The variables contained in d_i may differ from node to node based on the local sensing infrastructure. These can be complemented by other predictive variables that are available locally such as time or weather information. For illustration, we use a running example of a node that can measure only the local load p_i^c , the local PV generation p_i^g , and the present capacity \bar{s}_i . This yields the local training set with base variables and labels,

$$X_i = [d_i[1] \dots d_i[T]], Y_i = [u_i^*[1] \dots u_i^*[T]]. \quad (26)$$

The next step is to select a machine learning model that is expressive enough to reconstruct valid patterns in the optimal control actions that can be found in the local data, and that is simple enough to generalize well to new scenarios. We compared various model structures in our earlier work [37] and selected a multiple stepwise linear regression algorithm that selects a subset of available nonlinear features [17]. This model is linear in the parameters, but allows for nonlinear transformations of the base variables in $\varphi(d_i)$, concretely quadratic and interaction terms. For instance, if d_i contains 3 base variables as in our example, $\varphi(d_i)$ would yield 3 linear features; $\varphi_1^{(i)} := p_i^c$, $\varphi_2^{(i)} := p_i^g$ and $\varphi_3^{(i)} := \bar{s}_i$, and 6 more nonlinear features, of which 3 interaction terms ($\varphi_4^{(i)} := \varphi_1^{(i)} \varphi_2^{(i)}$ etc.) and 3 quadratic action terms ($\varphi_7^{(i)} := (\varphi_1^{(i)})^2$ etc.). In general, for B_i base variables, we construct $F_i = 2B_i + \binom{B_i}{2}$ features as inputs to the regression problem. The F_i input variables of the t^{th} sample are denoted as $\phi^{(i)}[t] \in \mathbb{R}^{F_i}$. All F_i features across all T data points can be organized as

$$\Phi^{(i)} = \begin{bmatrix} \phi^{(i)\top}[1] \\ \vdots \\ \phi^{(i)\top}[T] \end{bmatrix} = \begin{bmatrix} \varphi_1^{(i)}[1] & \dots & \varphi_{F_i}^{(i)}[1] \\ \vdots & \ddots & \vdots \\ \varphi_1^{(i)}[T] & \dots & \varphi_{F_i}^{(i)}[T] \end{bmatrix}. \quad (27)$$

We use a linear model to relate output Y_i to input matrix $\Phi^{(i)}$,

$$\hat{\pi}_i(\beta^{(i)}, \phi^{(i)}[t]) = \beta_0^{(i)} + \beta_1^{(i)} \varphi_1^{(i)}[t] + \dots + \beta_{F_i}^{(i)} \varphi_{F_i}^{(i)}[t]. \quad (28)$$

A least squares approach determines the coefficients $\beta^{(i)} = [\beta_0^{(i)}, \dots, \beta_{F_i}^{(i)}]$ that minimize the residuals sum of squares (29) given T samples,

$$\text{RSS}(\beta^{(i)}) = \sum_{t=1}^T \left(u_i^*[t] - \hat{\pi}(\beta^{(i)}, \phi^{(i)}[t]) \right)^2. \quad (29)$$

The algorithm is initialized with a multiple linear model of the basic variables in X_i only. At each iteration, the new feature that improves the Bayesian Information Criterion (BIC) [35] the most and sufficiently is added to the model. Subsequently, the variable with the lowest contribution is removed. These two steps are iterated until no variables meet the entrance or exit

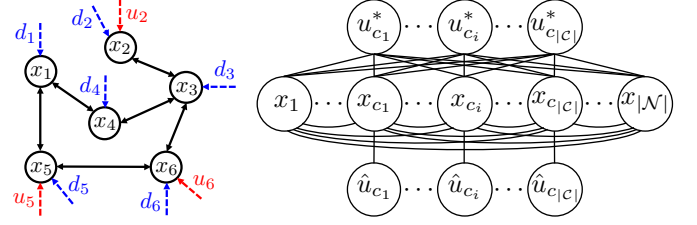


Fig. 1. (left) Distributed multi-agent problem. The circles denote the local state x_i of an agent, the dashed arrow denotes its inputs u_i (red) and disturbances d_i (blue), and the double arrows denote physical coupling between the state variables of different agents, (right) Markov Random Field (MRF) graphical model of the dependency structure of all variables in the decentralized learning problem. Note that the state variables x_i and the optimal actions u_i^* form a fully connected undirected network, and the local policy \hat{u}_i only depends on the local state x_i (which here includes disturbances d_i).

threshold of the algorithm. The goal of the stepwise selection algorithm is to select the subset of features that most accurately predicts the optimal power injection of a DER.

IV. RECONSTRUCTION AND COMMUNICATION

Rate Distortion Framework

As proposed in [15], we approach the problem of how well the decentralized policies $\hat{\pi}_i$ can perform in theory from the perspective of *rate distortion*. Rate distortion theory is a sub-field of information theory, which provides a framework for understanding and computing the minimal *distortion* incurred by any given *compression* scheme. For a detailed overview, see [12, Chapter 10]. In this context, we can interpret the fact that the output of each individual policy $\hat{\pi}_i$ depends only on the local state x_i as a compression of the full state x . We formulate our variant of the classical rate distortion problem

$$\begin{aligned} D^* &= \min_{p(\hat{u}|u^*)} \mathbb{E}[\mathbf{d}(\hat{u}, u^*)], \\ \text{s.t.} \quad & I(\hat{u}_i; u_j^*) \leq I(x_i; u_j^*) \triangleq \gamma_{ij}, \\ & I(\hat{u}_i; \hat{u}_j) \leq I(x_i; x_j) \triangleq \delta_{ij}, \forall i, j \in \mathcal{C}, \end{aligned} \quad (30)$$

where $I(\cdot, \cdot)$ denotes mutual information and $\mathbf{d}(\cdot, \cdot)$ an arbitrary non-negative distortion measure. The minimum distortion between random variable u^* and its reconstruction \hat{u} may be found by minimizing over conditional distributions $p(\hat{u}|u^*)$.

The novelty in (30) lies in the structure of the constraints. Typically, D^* is written as a function $D(R)$, where R is the maximum *rate* or mutual information $I(\hat{u}_i; u_i^*)$. From Fig. 1b however, we know that pairs of reconstructed and optimal actions cannot share more information than is contained in the intermediate nodes in the graphical model; \hat{u}_{c_1} and $u_{c_1}^*$ cannot share more information than x_{c_1} and $u_{c_1}^*$. This is a simple consequence of the data processing inequality [12, Thm. 2.8.1]. Similarly, the reconstructed optimal actions at two different nodes cannot be more closely related than the measurements x_i 's from which they are computed. The resulting constraints are fixed by the joint distribution of the state x and the optimal actions u^* ; they are fully determined by the structure of the optimization problem that we wish to solve (in our case (5)).

We emphasize that we have made virtually no assumptions about the distortion function. For the remainder of this paper,

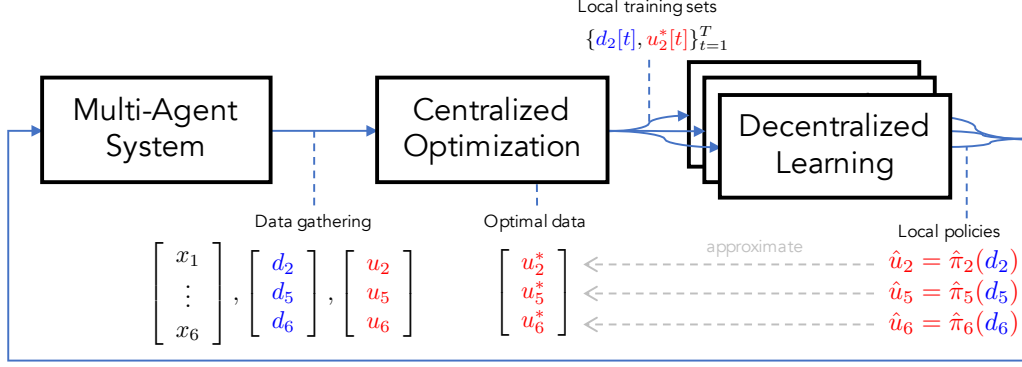


Fig. 2. A flow diagram explaining the key steps of the decentralized regression method, depicted for the example system in Fig. 1a. We first collect data from a multi-agent system, and then solve the centralized optimization problem using all the data. The data is then split into smaller training and test sets for all agents to develop individual decentralized policies $\hat{\pi}_i(x_i)$ (or $\hat{\pi}_i(d_i)$ as proposed in the context of OPF) that approximate the optimal solution of the centralized problem. These policies are then implemented in the multi-agent system to collectively achieve a common global behavior.

we will measure distortion as the mean square error (MSE) deviation between \hat{u}_i and u_i^* , which is a common *loss function* in supervised learning.

Allowing Restricted Communication

Suppose that a decentralized policy $\hat{\pi}_i$ suffers from insufficient mutual information between its local measurement x_i and the optimal action u_i^* . In this case, we would like to quantify the potential benefits of communicating with other nodes $j \neq i$ in order to reduce the distortion limit D^* from (30) and improve its ability to reconstruct u_i^* . Here, we build the information-theoretic solution to the problem of how to choose optimally which other data to observe, as proposed in [15]. We assume that in addition to observing its own local state x_i , each $\hat{\pi}_i$ is allowed to depend on at most k other $x_{j \neq i}$.

Lemma 1. (Restricted Communication [15])

If S_i is the set of k nodes $j \neq i \in \mathcal{N}$ which \hat{u}_i is allowed to observe in addition to x_i , then setting

$$S_i = \arg \max_{\mathcal{S}} I(u_i^*; x_i, \{x_j : j \in \mathcal{S}\}) : |\mathcal{S}| = k, \quad (31)$$

minimizes the best-case expectation of any distortion measure. That is, this choice of S_i yields the smallest lower bound D^* from (30) of any possible choice of \mathcal{S} .

Lemma 1 provides a means of choosing a subset of the state $\{x_j : j \neq i\}$ to communicate to each decentralized policy $\hat{\pi}_i$ that minimizes the corresponding best expected distortion D^* . Practically speaking, this result may be interpreted as formalizing the following intuition: “the best thing to do is to transmit the most information.” In this case, “transmitting the most information” corresponds to allowing $\hat{\pi}_i$ to observe the set \mathcal{S} of nodes $\{x_j : j \neq i\}$ which contains the most information about u_i^* . Likewise, by “best” we mean that S_i minimizes the best-case expected distortion D^* , for any distortion metric d . Without making some assumption about the structure of the distribution of x and u^* , we cannot guarantee that any particular regressor $\hat{\pi}_i$ will attain D^* . Nevertheless, in a practical situation where sufficient data $\{x[t], u^*[t]\}_{t=1}^T$ is available, we can solve (31) by estimating mutual information [20].

V. RESULTS FOR SINGLE-PHASE OPTIMAL POWER FLOW

We evaluate the proposed method on a realistic testbed that is constructed from two independent sources: we construct a 129 node feeder model based on a real distribution feeder from Arizona, Figure 3, and populate this with demand measurements [14]. Pecan Street power consumption and PV generation data with a resolution of 15 minutes is obtained from 126 individual residences in Austin, Texas for a period of 330 days. Individual household load and PV time series are selected randomly from the Pecan Street data set [14] and aggregated to match the spot load for each bus as specified in the experiment. We demonstrate Decentralized OPF through three experiments. The first experiment assumes controllable DER and loads spread randomly across a network. In this experiment, only reactive power is controlled with the objective to minimize voltage variations throughout the network. The second experiment considers a group of controllable DER concentrated in one area, and a group of large loads concentrated in another area. In this experiment, both real and reactive power are controlled and the objective is to produce power locally as much as possible. The third experiment aims to balance voltages across three phases in an unbalanced distribution system.

Case 1: Minimize Voltage Variations

For the first experiment, 50% of the 53 nodes with loads are randomly selected and equipped with PV installations with peak generation 80% of the peak real power load. We solve 2500 instances of OPF with sampled load and PV generation data to retrieve the optimal reactive power output of all inverters $\{u^*[t]\}_{t=1}^T$, with the objective set with $\alpha = 1, \beta = 2 \cdot 10^{-4}, \gamma = 0$. The data is separated into training, test and validation data. The test data is used to test the predictive performance of the machine learnine models. The obtained decentralized OPF controllers are then simulated on validation data.

For the case of no control, the voltage drop in the system is smallest between 10:00–16:00, when most real power demand is supplied by PV systems. The Decentralized OPF method achieves system voltages that are close to the nominal value of 1 p.u., and simultaneously reduces losses as implied by a

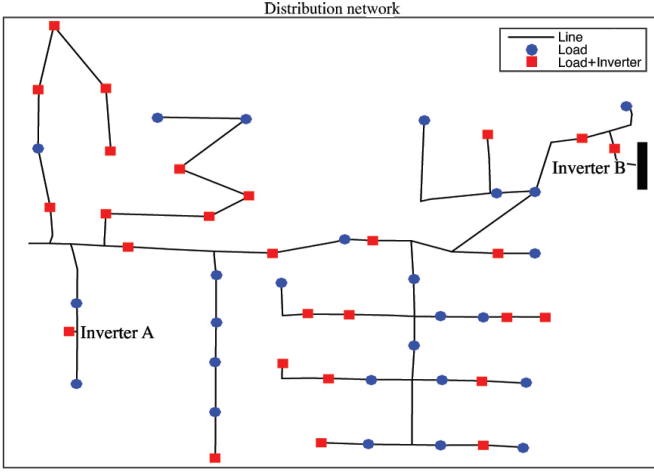


Fig. 3. Distribution feeder for scenario 1. Substation is located on the far left, locations of loads with PV inverters (squares), and without PV inverters (circles) are included.

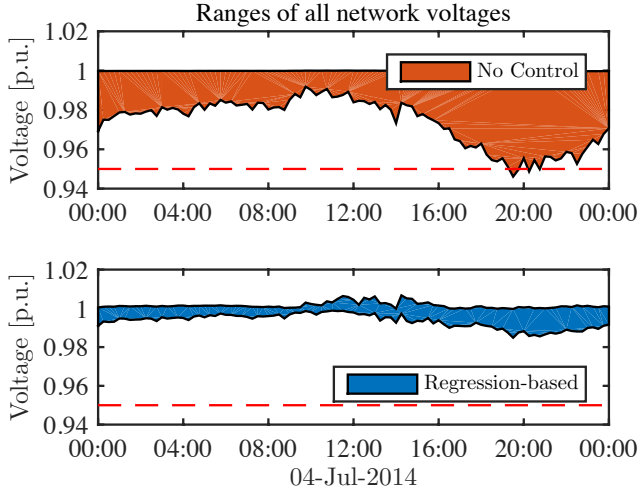


Fig. 4. All network voltages for the case of no control and applying the regression-based Decentralized OPF method. Colored planes represent the range between the maximum and minimum voltages at any node in the network. Lower voltage bound is indicated with red dashed line.

lower objective function value. The transition from peak PV generation to peak consumption between 12.00 and 20.00 causes the system voltage to change significantly without control. For the case of no control, the lower bound of the ANSI standard is violated in the evening if traditional voltage regulators are not operated. The effect of Decentralized OPF is obvious at these times: reactive power generated by inverters reduce voltage drop in the system and reduces losses. In addition to the comparison, we extended our method to show it is capable of collaboration with a load tap changer (LTC). We designed a scheme in which the DERs operate to flatten the voltage throughout the feeder. Once voltages are flattened, it is possible to simultaneously adjust the turn ratio of the LTC at the substation in order to safely lower voltage levels throughout the feeder [37].

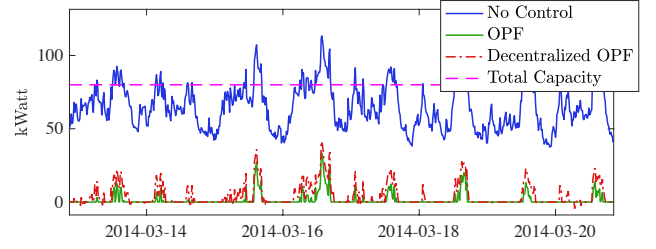


Fig. 5. Total net load delivered by the substation, in the case of: no control, OPF and Decentralized OPF.

Case 2: Localize Power Generation

Scenario 2 aims to show that the method also works for different power dynamics and objectives. We now assign 20 nodes in the lower right subradial with controllable DERs, see Figure 5. In addition, the spot loads of 12 nodes in the two left upper subradials are increased by a factor 3. By setting parameter γ in the objective function sufficiently high, this OPF problem tries minimize power procurement from the transmission grid by matching supply and demand locally, letting power flow from the area with controllable DER to the area with concentrated loads. The total real power capacity of the controllable DERs is assumed to be constant; future work will introduce time-varying capacity profiles based on charging, generation and consumption patterns. We assign 4 kWatt capacity to 20 inverters, totalling to 80 kWatt generation/consumption capacity across the feeder, as indicated by the dotted red line in Figure 5. Figure 5 shows how the decentralized OPF controllers elegantly mimic the centralized OPF solutions across the test data set. Notice how the power delivered by the substation is 0 for all times where the network's net load is smaller than the combined power capacity of 80 kWatt.

A. Case 3: Three-Phase Voltage Balancing

We also show the efficacy of Decentralized OPF for three-phase unbalanced networks, by learning and reconstructing the solutions $u_n^{p,\phi}, u_n^{q,\phi}$, with $\phi \in \{a, b, c\}$, of the centralized OPF problem (26), as formulated in Section 2 of the main paper. The feeder model used here is the IEEE 13 node test feeder [19]. Figure 6 shows the results of applying Decentralized OPF to balance voltage magnitudes across phases for a scenario with a significant gap between phase b and phase c of ≈ 0.1 p.u.. We see that the voltage magnitudes are tightly balanced across the network. Notice that in order to balance the large gap in the lower half of the feeder (nodes 671, 692, 675, 680, 684), a small increase in gap is incurred in the left upper radial (nodes 645, 646). Similar to the results for single-phase networks, the Decentralized OPF method also performs well at locally reconstructing OPF solutions in three-phase unbalanced networks, further validating its promise to serve as a new paradigm for regulating voltage and power flow in distribution networks.

VI. DISCUSSION

In Section VI-A, we analyze how the structure of different learned controllers $i, j \in \mathcal{C}$ differ across the network as reflected

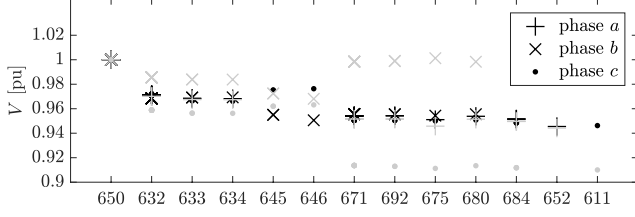


Fig. 6. Voltage magnitude balancing. In grey, voltage magnitudes across three phases without control. In black, voltage magnitudes across three phases applying decentralized OPF.

by parameters $\beta^{(i)}, \beta^{(j)}$ in (28). What does this tell us about the network and OPF problem? And secondly, in Section VI-B, we analyze how the optimal communication strategy, as determined via Lemma 1 and (31), differs between scenario 1 and 2. Lastly, in Section VI-C, we discuss practical considerations to integrate the decentralized OPF method across distribution planning and operation.

A. Interpreting the Machine Learning Models

In our case study, we determined regression models for 27 different inverters. Table I shows regression results for inverters A and B (both indicated in Figure 3). The first two columns present the features selected by the stepwise regression and the values for the β -coefficients in (28). The third column shows the standard error of the estimate, and the fourth lists p-values, which here means the probability that coefficient is zero. A p-value of 0.1 implies a 10% chance that the corresponding coefficient is zero. Note how the stepwise regression approach results in two clearly different models. The reactive power output of inverter A depends predominantly on the local reactive power consumption $\varphi_2^{(A)}$, while the output of inverter B is strongly related to the reactive power capacity $\varphi_3^{(B)}$ and $\varphi_2^{(B)}$ is less relevant. Inverter A's structure can be explained by the fact it is located at the end of the feeder. As a result, the aggregate power flow at A is relatively low and correlated with A's own consumption. As the objective is to minimize losses and voltage deviations, A tries to produce a signal that looks like providing the neighboring demand for reactive power, thereby minimizing current locally and upstream. Inverter B's structure can be explained by its location close to the feeder head. In this area, the aggregate power flow is much larger, and the output of inverter B is needed more as a "bulk" product to lower the flow on branches elsewhere in the network. This causes inverter B to operate at its maximum capacity most of the time, causing correlation with the output. As the maximum capacity varies with the local real power generation at B (a constraint formulated in (11)), the learning algorithm tries to "listen closely" to the present maximum capacity. This example illustrates that optimal reactive power output of two inverters can have a completely different structure. Therefore, effective design of controllers based on local measurements is challenging, and can benefit from a data driven approach.

TABLE I
NORMALIZED REGRESSION COEFFICIENTS FOR INVERTER A AND B, AS DEPICTED IN FIGURE 3.

A	Est.	SE	p-value	B	Est.	SE	p-value
offset	0.02	0.01	0.01	offset	0.02	0.00	$8.2e^{-4}$
φ_1	0.37	0.01	0	φ_1	0.04	0.00	$3.2e^{-22}$
φ_2	0.77	0.01	0	φ_3	0.96	0.01	0
φ_3	-0.21	0.02	$8.0e^{-24}$	$\varphi_1\varphi_3$	0.06	0.01	$1.2e^{-12}$
$\varphi_1\varphi_2$	0.17	0.01	0	φ_1^2	-0.03	0.00	$3.9e^{-14}$
φ_1^2	-0.06	0.01	$1.4e^{-12}$	φ_3^2	-0.03	0.01	$6.1e^{-9}$

B. The Effect of Communication

The ability to fully decentralize OPF problems is surprising. The information theoretic lens used in this paper complements insights from control-theoretic analysis that show the necessity of communication for a large class of local controllers to ensure equilibria are feasible with respect to voltage constraints [11]. In our setting, the use of exogenous disturbance variables d_i prevents the need for a dynamic analysis as d_i is not affected by the control signals. Rather than for the purpose of stability and feasibility, in [15], we applied Lemma 1 to the OPF problem for a smaller network [19], in order to study the value of communication for improving the reconstruction of u^* , yielding an optimal communication strategy. In this paper, we also studied the emerging communication topology that arises from maximizing the mutual information between the optimal actions and the combined available measured variables. For case 1, where we minimize voltage deviations and losses across the network with DERs spread randomly across all buses, we see no particular patterns in the optimal communication infrastructure. Some DERs closer to the end of the network tend to communicate with loads nearby, which is explained by the emerging effect in OPF supply tends to match demand nearby to minimize losses higher upstream in the radial network. For case 2, where we are localizing the production of power by minimizing the power delivered from the substation, and interesting pattern arises from the fact that the loads and DER are concentrated in different areas. As a result, if we allow DERs to observe one extra node anywhere in the network, all select a node in the area with concentrated loads. This makes intuitive sense as the optimal control actions are largely responding to the high demand in the other area. In addition, across all 20 DERs the selected nodes are all in a set of only 3 nodes, suggesting an efficient sensor implementation.

C. Designing Across Planning and Operation

An important practical consideration of implementing control schemes for active distribution networks is the impact on the planning and operation processes. Recent work has considered the co-optimization of planning and operation by considering both traditional expansion measures (such upgrading transformers or cables) as well as real-time control through DES, utilizing a decision-making process that builds on an iterative AC optimal power flow method [21, 22].

When using supervised learning, some immediate concerns arise around the quality of the training set and the historical

data used to construct it. Firstly, a designer wants to have certainty that the historical data reflect the “normal” system behavior expected in future operation. If certain scenarios are not measured historically, the controllers may not *learn* how to respond in an optimal or desired way. If future scenarios are not measured, but can be anticipated, it may be possible to instead *simulate* these and augment these to the historical data. Secondly, a designer might want to know what happens when something changes in the system, such as a new street block connecting to a feeder or the installation of new electric vehicles or other DERs. This concern is valid for any controller. In our future work, we are assessing different learning-based controllers for OPF on their performance across a spectrum of system changes. Again, if some of these changes are anticipated by a planning process, it may be possible to simulate these changes. By adding these to the training set, controllers may learn to *anticipate* these. Otherwise, for smaller changes, a periodic retraining procedure can update the control parameters incrementally by adding new historical measurements.

VII. CONCLUSIONS

In this paper, we presented an integrative approach for decentralizing optimal power flow methods based on machine learning. A rate distortion framework allowed to interpret the decentralized learning approach as a compression and reconstruction problem, providing a theoretical lower bound on the distortion that can be achieved with local information and a procedure to improve controllers by communicating with a node that maximizes the mutual information between the optimal control and the available variables. Experiments on both single- and three-phase unbalanced (see supplementary material) systems illustrated the relevancy of Decentralized OPF for a broad range of systems and objectives. The machine learning models provide new insights into complex power networks to understand the behavior of individual inverters in OPF implementations and their need for communication. Lastly, we pointed at some open problems toward practical integration in the planning and operation of distribution grids.

ACKNOWLEDGMENTS

We thank Michael Sankur for contributions to the code base for this work. This work is supported by the National Science Foundation’s CPS FORCES Grant (award number CNS-1239166) and the UC-Philippine-California Advanced Research Institute (award number IIID-2015-10).

REFERENCES

- [1] D. B. Arnold et al. “Model-free optimal control of var resources in distribution systems: An extremum seeking approach”. In: *IEEE Transactions on Power Systems* 31.5 (2016), pp. 3583–3593.
- [2] D. B. Arnold et al. “Optimal dispatch of reactive power for voltage regulation and balancing in unbalanced distribution systems”. In: *16th IEEE Power & Energy Society General Meeting (PESGM)*. IEEE Power & Energy Society General Meeting (PESGM). IEEE, 2016.
- [3] X. Bai et al. “Semidefinite programming for optimal power flow problems”. In: *International Journal of Electrical Power & Energy Systems* 30.6 (2008), pp. 383–392.
- [4] M. Baran and F. Wu. “Optimal capacitor placement on radial distribution systems”. In: *IEEE Transactions on Power Delivery* 4.1 (Jan. 1989), pp. 725–734.
- [5] M. E. Baran and F. F. Wu. “Optimal sizing of capacitors placed on a radial distribution system”. In: *Power Delivery, IEEE Transactions on* 4.1 (1989), pp. 735–743.
- [6] F. Bellizio et al. “Optimized local control schemes for active distribution grids using machine learning techniques”. In: *Submitted to IEEE PES GM*. Nov. 2017.
- [7] S. Bolognani and F. Dörfler. “Fast scenario-based decision making in unbalanced distribution networks”. In: *2016 Power Systems Computation Conference (PSCC)*. 2016 Power Systems Computation Conference (PSCC). June 2016, pp. 1–7.
- [8] S. Bolognani and S. Zampieri. “A Distributed Control Strategy for Reactive Power Compensation in Smart Microgrids”. In: *IEEE Transactions on Automatic Control* 58.11 (Nov. 2013), pp. 2818–2833.
- [9] V. Calderaro et al. “Optimal decentralized voltage control for distribution systems with inverter-based distributed generators”. In: *Power Systems, IEEE Transactions on* 29.1 (2014), pp. 230–241.
- [10] P. M. Carvalho, P. F. Correia, and L. A. Ferreira. “Distributed reactive power generation control for voltage rise mitigation in distribution networks”. In: *IEEE Transactions on Power Systems* 23.2 (2008), pp. 766–772.
- [11] G. Cavraro et al. “The value of communication in the voltage regulation problem”. In: *Decision and Control (CDC), 2016 IEEE 55th Conference on*. IEEE, 2016, pp. 5781–5786.
- [12] T. M. Cover and J. A. Thomas. *Elements of information theory*. John Wiley & Sons, 2012.
- [13] E. Dall’Anese, H. Zhu, and G. Giannakis. “Distributed Optimal Power Flow for Smart Microgrids”. In: *IEEE Transactions on Smart Grid* 4.3 (Sept. 2013), pp. 1464–1475.
- [14] *Dataport*. Pecan Street Inc. Dataport. 2017. URL: <http://www.pecanstreet.org/>.
- [15] R. Dobbe, D. Fridovich-Keil, and C. Tomlin. “Fully Decentralized Policies for Multi-Agent Systems: An Information Theoretic Approach”. In: *Conference on Neural Information Processing Systems*. Long Beach, CA, USA, Dec. 2017.
- [16] M. Farivar et al. “Optimal inverter VAR control in distribution systems with high PV penetration”. In: *Power and Energy Society General Meeting, 2012 IEEE*. IEEE, 2012, pp. 1–7.
- [17] J. Friedman, T. Hastie, and R. Tibshirani. *The elements of statistical learning*. Vol. 1. Springer series in statistics Springer, Berlin, 2001.
- [18] L. Gan and S. H. Low. “Convex relaxations and linear approximation for optimal power flow in multiphase radial networks”. In: *Power Systems Computation Conference*. Aug. 2014.

- [19] *IEEE Distribution Test Feeders*. Distribution Test Feeders. 2017. URL: <http://ewh.ieee.org/soc/pes/dsacom/testfeeders/>.
- [20] J. Jiao et al. "Minimax Estimation of Functionals of Discrete Distributions". In: *arXiv preprint* (June 26, 2014). arXiv: 1406.6956.
- [21] S. Karagiannopoulos, P. Aristidou, and G. Hug. "Co-optimisation of planning and operation for active distribution grids". In: *PowerTech*. Manchester, UK: IEEE, 2017.
- [22] S. Karagiannopoulos, P. Aristidou, and G. Hug. "Hybrid approach for planning and operating active distribution grids". In: *IET Generation, Transmission & Distribution* 11.3 (2017), pp. 685–695.
- [23] A. Keane et al. "Enhanced utilization of voltage control resources with distributed generation". In: *IEEE Transactions on Power Systems* 26.1 (2011), pp. 252–260.
- [24] S. Lacey and R. Hanley. *The Interchange Podcast with Ryan Hanley: Building a Blueprint for the Transactive Grid at PG&E, SolarCity, Tesla and AMS*. Green Tech Media. Mar. 6, 2018. URL: <https://www.greentechmedia.com/articles/read/the-blueprint-for-the-distributed-grid> (visited on 03/31/2018).
- [25] J. Lavaei and S. Low. "Zero Duality Gap in Optimal Power Flow Problem". In: *IEEE Transactions on Power Systems* 27.1 (Feb. 2012), pp. 92–107.
- [26] N. Li, G. Qu, and M. Dahleh. "Real-time decentralized voltage control in distribution networks". In: *Communication, Control, and Computing (Allerton), 2014 52nd Annual Allerton Conference on*. IEEE, 2014, pp. 582–588.
- [27] R. Louca, P. Seiler, and E. Bitar. "Nondegeneracy and inexactness of semidefinite relaxations of optimal power flow". In: *arXiv preprint arXiv:1411.4663* (2014).
- [28] S. Low. "Convex Relaxation of Optimal Power Flow; Part I: Formulations and Equivalence". In: *IEEE Transactions on Control of Network Systems* 1.1 (Mar. 2014), pp. 15–27.
- [29] J. A. Momoh et al. "Challenges to optimal power flow". In: *IEEE Transactions on Power Systems* 12.1 (Feb. 1997), pp. 444–455.
- [30] B. Robbins, C. Hadjicostis, and A. Dominguez-Garcia. "A Two-Stage Distributed Architecture for Voltage Control in Power Distribution Systems". In: *IEEE Transactions on Power Systems* 28.2 (May 2013), pp. 1470–1482.
- [31] B. A. Robbins and A. D. Dominguez-Garcia. "Optimal reactive power dispatch for voltage regulation in unbalanced distribution systems". In: *IEEE Transactions on Power Systems* 31.4 (2016), pp. 2903–2913.
- [32] K. M. Rogers et al. "An authenticated control framework for distributed voltage support on the smart grid". In: *IEEE Transactions on Smart Grid* 1.1 (2010), pp. 40–47.
- [33] M. Sankur et al. "A Linearized Power Flow Model for Optimization in Unbalanced Distribution Systems". In: *arXiv preprint arXiv:1606.04492* (2016).
- [34] M. Sankur et al. "Optimal Voltage Phasor Regulation for Switching Actions in Distribution Systems". In: *IEEE Transaction on Smart Grids* (Under Review) (Apr. 2018).
- [35] G. Schwarz. "Estimating the dimension of a model". In: *The annals of statistics* 6.2 (1978), pp. 461–464.
- [36] J. Smith et al. "Smart inverter volt/var control functions for high penetration of PV on distribution systems". In: *Power Systems Conference and Exposition (PSCE), 2011 IEEE/PES*. Power Systems Conference and Exposition (PSCE), 2011 IEEE/PES. Mar. 2011, pp. 1–6.
- [37] O. Sondermeijer et al. "Regression-based Inverter Control for Decentralized Optimal Power Flow and Voltage Regulation". In: *Power & Energy Society General Meeting*. Boston, MA, USA: IEEE, July 2016.
- [38] E. Stewart et al. *Analysis of High-Penetration Levels of Photovoltaics into the Distribution Grid on Oahu, Hawaii: Detailed Analysis of HECO Feeder WF1*. National Renewable Energy Laboratory (NREL), Golden, CO., 2013.
- [39] P. Šulc, S. Backhaus, and M. Chertkov. "Optimal distributed control of reactive power via the alternating direction method of multipliers". In: *IEEE Transactions on Energy Conversion* 29.4 (2014), pp. 968–977.
- [40] K. Turitsyn et al. "Options for Control of Reactive Power by Distributed Photovoltaic Generators". In: *Proceedings of the IEEE* 99.6 (June 2011), pp. 1063–1073.
- [41] B. Zhang, A. D. Dominguez-Garcia, and D. Tse. "A local control approach to voltage regulation in distribution networks". In: *North American Power Symposium (NAPS)*. IEEE, 2013.
- [42] B. Zhang et al. "An Optimal and Distributed Method for Voltage Regulation in Power Distribution Systems". In: *IEEE Transactions on Power Systems* 30.4 (July 2015), pp. 1714–1726.